

## LETTERS

## Experimental purification of two-atom entanglement

R. Reichle<sup>1</sup>†, D. Leibfried<sup>1</sup>, E. Knill<sup>1</sup>, J. Britton<sup>1</sup>, R. B. Blakestad<sup>1</sup>, J. D. Jost<sup>1</sup>, C. Langer<sup>1</sup>, R. Ozeri<sup>1</sup>, S. Seidelin<sup>1</sup> & D. J. Wineland<sup>1</sup>

Entanglement is a necessary resource for quantum applications—entanglement established between quantum systems at different locations enables private communication<sup>1</sup> and quantum teleportation<sup>2</sup>, and facilitates quantum information processing<sup>3</sup>. Distributed entanglement is established by preparing an entangled pair of quantum particles in one location, and transporting one member of the pair to another location. However, decoherence during transport reduces the quality (fidelity) of the entanglement. A protocol to achieve entanglement ‘purification’ has been proposed<sup>4</sup> to improve the fidelity after transport. This protocol uses separate quantum operations at each location and classical communication to distil high-fidelity entangled pairs from lower-fidelity pairs. Proof-of-principle experiments distilling entangled photon pairs have been carried out<sup>5–9</sup>. However, these experiments obtained distilled pairs with a low probability of success and required destruction of the entangled pairs, rendering them unavailable for further processing. Here we report efficient and non-destructive entanglement purification<sup>4</sup> with atomic quantum bits. Two noisy entangled pairs were created and distilled into one higher-fidelity pair available for further use. Success probabilities were above 35 per cent. The many applications of entanglement purification make it one of the most important techniques in quantum information processing.

Recent efforts to realize practical quantum information processing devices based on various physical systems have led to impressive new developments<sup>10</sup>. Much-anticipated applications of quantum information processing devices are quantum communication and quantum computing. Large-scale implementations require distributing each quantum bit (qubit) of an entangled pair of qubits to separate locations. In quantum communication, entangled pairs are the fundamental resource for quantum teleportation<sup>2</sup>, entanglement-based quantum cryptography<sup>1</sup> and other protocols. They also underlie several promising schemes for quantum computing<sup>3,11</sup>, are needed for fast coupling of distant qubits<sup>12,13</sup> and play an important part in recent methods for achieving fault-tolerance<sup>14</sup>. In all applications, it is important to ensure high fidelity of the entangled pairs once they are distributed to their destinations. This is particularly difficult in quantum communication, because most schemes require conversion between stationary (usually material) qubits suitable for storage or manipulation and ‘flying’ (usually photonic) qubits suitable for transport.

To restore fidelity lost during transport of entangled qubits, we can use entanglement purification<sup>4</sup> to distil a smaller number of high-fidelity entangled qubits. The simplest instance of the entanglement purification protocol of ref. 4 distils one entangled pair of qubits from two imperfectly entangled ones. Here the qubits at one location are compared by means of local quantum operations. The results of the comparison are shared through classical communication between locations, and if they are consistent, a higher-fidelity pair of entangled qubits is obtained. Assuming no error in the comparison and

sufficiently entangled initial pairs, the process can be iterated in multiple ‘rounds’ to obtain arbitrarily high-fidelity entangled pairs. Previous experiments, using photons, included demonstrations of entanglement purification<sup>6,9</sup> and entanglement concentration<sup>5,7,8</sup>, which required specific input states. However, in these experiments, entangled pairs were obtained by post-selection with a low success probability of  $<10^{-3}$  per try. As two pairs are needed for an experiment, purification success probabilities were less than  $10^{-6}$  per try. In addition, successful comparisons required destruction of entanglement, so the purified entangled pairs were not available for further use.

Here we report experiments that faithfully implemented the purification protocol proposed in ref. 4. An important feature of this protocol is that it works for all input states with sufficient fidelity with respect to the desired ideal entangled state. We tested the protocol on a family of input states that are approximately pure. Although other methods such as entanglement concentration can achieve better fidelity for our input states, this is at the cost of lower success probability, and our goal was to demonstrate a purification

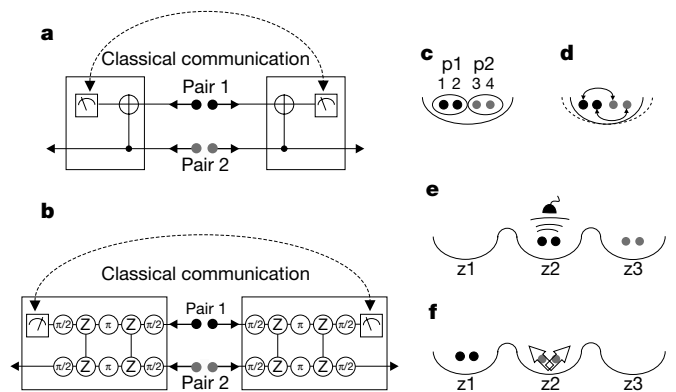


**Figure 1 | Network diagrams for purification.** **a**, The original proposal<sup>4</sup>. The qubits of both pairs are connected by CNOT gates across the pairs, after which the two qubits of pair 1 are measured. The measurement outcomes are compared by classical communication, and purification succeeds if they are the same. **b**, Experimental implementation in this work. The ion qubits of both entangled pairs are (1) rotated by  $R(\pi/2, \pi/4)$  (see Methods), (2) connected by two-ion  $\varepsilon = \pi/4$ -phase gates across the pairs (marked with Z), (3) rotated by  $R(\pi, 5\pi/4)$ , (4) connected by two-ion  $\varepsilon = \pi/4$ -phase gates again and (5) finally rotated by  $R(\pi/2, \pi/4)$ . The ions of pair 1 are then measured, and purification succeeds if the two measurement outcomes are different. **c–f**, Gates applied to ions and positions of the ions. The potential well zones are shown schematically under the ions. **c**, With all ions trapped in one potential well, entangled pair p1 (black) and pair p2 (grey) are created by a phase gate as described in Methods. **d**, Corresponding ions in each pair are connected by phase gates (as shown in **b**). **e**, The pairs are separated into zones z2 and z3, and p1 is measured by state-dependent fluorescence. **f**, After moving the ions, the fidelity of p2 is determined in z2 by state tomography.

<sup>1</sup>National Institute of Standards and Technology, Boulder, Colorado 80305, USA. †Present address: University of Ulm, 89069 Ulm, Germany.

protocol that is in principle useful for any sufficiently entangled input state. By randomizing the data for different input states, we determined the success of the protocol on effectively mixed states, a technique also used in ref. 6. We deterministically produced entangled pairs of  ${}^9\text{Be}^+$  atomic ion qubits that were then distilled. The protocol succeeded with probabilities between 35% and 65%, depending on the initial fidelity. We demonstrated a gain in fidelity for a range of initial fidelities. In principle, the purified pairs are available for further rounds of the purification protocol or for use in other algorithms.

Our experimental procedure follows the original proposal of ref. 4 that is shown in Fig. 1a. We first confined four  ${}^9\text{Be}^+$  ions in one trapping zone of a linear multi-zone Paul trap<sup>15</sup> where they formed a linear array along the weakest axis of the trapping potential (Fig. 1c), which was approximately harmonic in three dimensions. Qubits were implemented with two hyperfine ground states of each ion,  $|F=1, m_F=-1\rangle$  and  $|F=2, m_F=-2\rangle$ , designated respectively  $|\uparrow\rangle$  and  $|\downarrow\rangle$  for simplicity. We implemented qubit rotations  $R(\theta, \phi)$  (see Methods) by driving stimulated Raman transitions with two laser fields<sup>15</sup>. Multi-qubit operations were realized with geometric phase gates generalized from the two-qubit phase gate described in ref. 16 (see Methods).

To prepare the initial state of the four-qubit register, all four modes of motion of the linear array were cooled to the ground state<sup>17</sup>, and the internal qubit states were optically pumped to  $|\downarrow\rangle$ . We then generated two pairs of qubits with varying degrees of entanglement, as depicted schematically in Fig. 1c. A phase gate embedded between rotations on all ions entangled pair 1 (p1, consisting of ions 1 and 2) and pair 2 (p2, consisting of ions 3 and 4) separately at the same time, while all four ions were held in the same trap potential well. Ideally, after this operation the state of the two pairs is:

$$|\Phi\rangle_{p1} \otimes |\Phi\rangle_{p2} = (\cos(\varepsilon)|\downarrow\downarrow\rangle_{12} + i\sin(\varepsilon)|\uparrow\uparrow\rangle_{12}) \otimes (\cos(\varepsilon)|\downarrow\downarrow\rangle_{34} + i\sin(\varepsilon)|\uparrow\uparrow\rangle_{34}) \quad (1)$$

For angle  $\varepsilon = \pi/4$ , the state is a product of two maximally entangled Bell pairs  $|\Phi_{\text{Bell}}\rangle_j = \frac{1}{\sqrt{2}}(|\downarrow\downarrow\rangle_j + i|\uparrow\uparrow\rangle_j)$ , with  $j = \{p1, p2\}$ . Experimentally, the states  $|\Phi\rangle_j$  were obtained with a fidelity of approximately 0.75 for  $\varepsilon = \pi/4$ , limited by imperfections in the phase gate operation. Ideally, for general  $\varepsilon$ , the fidelity of each of the created pairs with respect to this Bell pair is:

$$F_{\text{pair}} = \left| \langle \Phi | \Phi_{\text{Bell}} \rangle_j \right|^2 = \cos^2(\varepsilon - \pi/4) \quad (2)$$

The states  $|\Phi\rangle_j$  can be viewed as the ideal Bell pairs ( $\varepsilon = \pi/4$ ) perturbed by a coherent combination of phase (sign flip) errors for  $\varepsilon \neq \pi/4$ . To lowest order in the deviation of  $\varepsilon$  from  $\pi/4$ , the errors act on just one of the qubits and are detectable by the purification process. By applying the purification protocol to this family of states, we are able to determine how well the experimental implementation performs on this type of phase error. To determine the performance on mixtures of these states, we use weighted combinations of the data for different  $\varepsilon$ .

We implemented a slight variation of the ref. 4 proposal shown in Fig. 1b. We used one purification phase gate connecting each member of the first entangled pair to its counterpart in the second pair (Fig. 1d). The first two qubits (p1) were then measured to determine whether purification succeeded (Fig. 1e). Execution of the phase gate ideally results in the state:

$$|\Psi\rangle = \frac{1}{2}(|\downarrow\uparrow\rangle_{12}|\downarrow\uparrow\rangle_{34} + |\uparrow\downarrow\rangle_{12}|\uparrow\downarrow\rangle_{34} + \cos(2\varepsilon)(|\downarrow\downarrow\rangle_{12}|\downarrow\downarrow\rangle_{34} + |\uparrow\uparrow\rangle_{12}|\uparrow\uparrow\rangle_{34}) + \sin(2\varepsilon)(|\downarrow\uparrow\rangle_{12}|\uparrow\downarrow\rangle_{34} + |\uparrow\downarrow\rangle_{12}|\downarrow\uparrow\rangle_{34}) \quad (3)$$

The quantum correlations between the entangled pairs are similar to those produced in the original proposal. However, measurement on

the first two qubits must show they are either  $|\uparrow\downarrow\rangle$  or  $|\downarrow\uparrow\rangle$  for the purification to succeed, and the resulting entangled state of qubits 3 and 4 is then rotated such that when  $\varepsilon = \pi/4$  the state is  $|\Psi_+\rangle \equiv \frac{1}{\sqrt{2}}(|\uparrow\downarrow\rangle + |\downarrow\uparrow\rangle)$ . For general  $\varepsilon$ , the probability of measuring that ions 1 and 2 are different is  $P_s = \frac{1}{2}[1 + \sin^2(2\varepsilon)]$ , in which case the state of the second pair of qubits is projected to:

$$|\Psi_{\text{purif}}\rangle = \frac{1}{\sqrt{1 + \sin^2(2\varepsilon)}} \times \begin{cases} (|\uparrow\downarrow\rangle + \sin(2\varepsilon)|\downarrow\uparrow\rangle) & \text{for first pair in } |\uparrow\downarrow\rangle \\ (|\downarrow\uparrow\rangle + \sin(2\varepsilon)|\uparrow\downarrow\rangle) & \text{for first pair in } |\downarrow\uparrow\rangle \end{cases} \quad (4)$$

Ideally, the purified fidelity is independent of whether  $|\uparrow\downarrow\rangle$  or  $|\downarrow\uparrow\rangle$  is detected and:

$$F_{\text{purif}} = |\langle \Psi_{\text{purif}} | \Psi_+ \rangle|^2 = \frac{4 \cos^4(\varepsilon - \pi/4)}{3 + \cos[4(\varepsilon - \pi/4)]} \geq F_{\text{pair}} \quad (0 \leq \varepsilon \leq \pi/2) \quad (5)$$

Near  $\varepsilon = \pi/4$ , the fidelity of the unpurified pairs decreases quadratically in  $(\varepsilon - \pi/4)$ , whereas the fidelity of the purified pair decreases quartically.

For the measurements and determination of the fidelity of the purified pair, we separated groups of ions in the multi-zone architecture of the trap<sup>15</sup>. We chose an order of the ions that made the measurement on p1 and the subsequent tomography on p2 as simple as possible. If we were distilling remote entanglement, then both pairs p1 and p2 would have one qubit in each location. Results of the

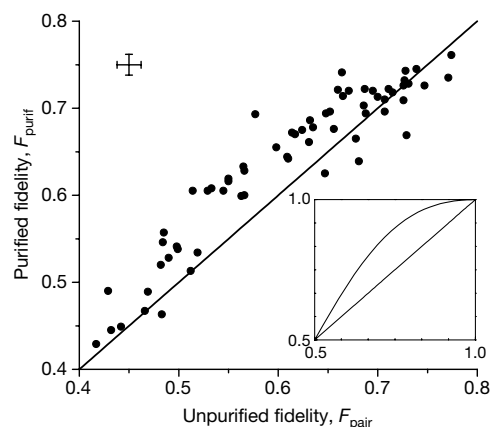


**Figure 2 | Purified fidelity as a function of unpurified fidelity.** The solid straight line in the main figure and inset represents  $F_{\text{pair}} = F_{\text{purif}}$ . For the experimental data points,  $F_{\text{pair}}$  was varied by experimentally setting angles  $0 \leq \varepsilon \leq \pi/4$  to (ideally) obtain entangled pairs described by equation (1). Both fidelities were determined by (partial) state tomography on pair 2 as depicted in Fig. 1f, and are given by the probability that the pair was in state  $|\Psi_+\rangle = \frac{1}{\sqrt{2}}(|\uparrow\downarrow\rangle + |\downarrow\uparrow\rangle)$ . For determining the unpurified fidelity, each purification experiment was immediately followed by an experiment that was identical except for the omission of the purifying gate, which are the operations inside the boxes of Fig. 1b. A rotation  $R(\pi/2, -\pi/4)$ , transforming  $|\Phi_{\text{Bell}}\rangle$  into  $|\Psi_+\rangle$ , was applied to both pairs instead. The standard error of the points is approximately 0.012 in both variables (see representative error bars shown in the graph), as estimated by resampling (see Methods). The scatter in the points, caused by drifts in experimental conditions, significantly exceeds this standard error (see Methods). The curved solid line in the inset shows the theoretical purified fidelity as a function of the input pair fidelity for the demonstrated protocol and perfect operations as expressed by equations (2) and (5). Axis designations are the same as for the main plot. For a mixture of our data that approximates a uniform distribution of angles  $\varepsilon$  in equation (1) between  $\varepsilon = 0$  and  $\varepsilon = \pi/4$ , we obtained an unpurified fidelity of  $0.614 \pm 0.0015$ , and a purified fidelity of  $0.629 \pm 0.0015$ . This implies a statistically significant improvement in fidelity of  $0.015 \pm 0.002$  for this particular mixture.

measurement on p1 would then have to be communicated between the locations (as depicted in Fig. 1a) to compare the local outcomes.

All ions were transferred into a separation zone and separated into the two initial pairs within 380  $\mu\text{s}$ . Pair p1 returned to the original interaction zone, where the state of the two ions was detected by state-dependent fluorescence (Fig. 1e). We used a detection period of 200  $\mu\text{s}$ , during which we detected about 0.5 photons if both ions were in state  $|\uparrow\rangle$ , and about 10 photons on average for each ion in state  $|\downarrow\rangle$ . We declared the purification a success when the number of counts was in an interval determined by the property that the probability of falsely declaring success with both ions in state  $|\uparrow\rangle$  ( $|\downarrow\rangle$ ) was less than 0.01 (0.05). We then moved pair p1 out of the interaction zone and the purified pair p2 into it (Fig. 1f) in about 470  $\mu\text{s}$ . The state of p2 was analysed by a tomography procedure that determined all four Bell-state populations without distinguishing between the ions. This yielded an experimental value of the fidelity  $F_{\text{purif}}$  (see Methods). The complete experimental sequence, including tomography, took about 1.54 ms.

For comparison, each attempt at purification was followed by a reference experiment in which the entangled pairs were prepared in the same way but the purification phase gate was omitted. Instead we applied a common rotation  $R(\pi/2, -\pi/4)$  to both pairs, transforming  $|\Phi_{\text{Bell}}\rangle$  into  $|\Psi_{+}\rangle$ . The fidelity  $F_{\text{pair}}$  of pair p2 was then determined by the same tomography procedure. The fidelity of p1 was characterized in separate experiments and found to be equal to that of p2 within experimental uncertainties. Therefore  $F_{\text{pair}}$  is the fidelity of a prepared Bell pair if purification was not used. The same noise processes act on the ions in the purification and the reference experiment after the time in the procedure where the purification gate would be applied. To determine the effectiveness of purification,  $F_{\text{pair}}$  was compared to  $F_{\text{purif}}$  (Fig. 2). The final fidelity of the purified pair reached a maximum of about 0.75. Nevertheless, we demonstrated an improvement  $F_{\text{purif}} > F_{\text{pair}}$  for  $0.5 \leq F_{\text{pair}} \leq 0.7$ . Ideally, neither fidelity should drop below 0.5 for the family of states used here. The apparent improvements discernible in the figure for  $F_{\text{pair}} < 0.5$  are explained by the common sources of errors equally affecting the purification and reference experiments after the time when the purification gate is implemented (or not). Depending on the initial fidelity, the probability of success varied between 35% and 65%.

The data shown in Fig. 2 are for the family of states given in equation (1) perturbed by experimental noise. From this data, one can infer the performance of the purification protocol on mixtures of such states. We chose a mixture that approximates a uniform distribution of angles  $\varepsilon$  in equation (1) between  $\varepsilon = 0$  and  $\varepsilon = \pi/4$ . The unpurified fidelity for this mixture was  $0.614 \pm 0.0015$ , and the purified fidelity was  $0.629 \pm 0.0015$ . This implies a statistically significant improvement in fidelity of  $0.015 \pm 0.002$  for this particular mixture.

As the purification protocol took place with the two pairs in the same trapping zone and with operations simultaneously acting on all ions, it was necessary to verify that the implemented operations did not introduce unintended correlations. We confirmed experimentally that, subject to the limitations of the tomographic analysis, state preparation resulted in independent pairs of entangled ions and, if the purification gate was applied directly to the state  $|\uparrow\uparrow\uparrow\uparrow\rangle$  or  $|\downarrow\downarrow\downarrow\downarrow\rangle$ , the state of ions 1 and 3 was independent of the state of ions 2 and 4, within experimental error.

Thresholds of tolerable error rates for entanglement purification in quantum repeaters are of the order of a few per cent, much less than the imperfections present in our current experiment. To improve state preparation and purification in future implementations, better control of classical parameters such as magnetic field and laser intensity will be required. Decoherence due to spontaneous emission could be reduced by an appropriate choice of the laser-beam detuning<sup>18</sup>. More advanced multi-zone traps and sympathetic cooling<sup>19</sup> will make it possible to implement purification with the ions of each entangled pair transported to separated trap zones. With these improvements, purified Bell pairs with sufficient fidelity to violate

Bell inequalities should be feasible. Because the two pairs of entangled states in equation (1) have identical angles  $\varepsilon$ , our procedure tests the behaviour of the purification protocol in the case of collective phase errors. To determine the behaviour for other phase errors, one could use individual laser addressing of the ion or magnetic field gradients.

In summary, we have demonstrated entanglement purification with relatively high success rates in a potentially scalable system. The protocol and success rates demonstrated, together with the availability of the purified pair, could enable ‘entanglement pumping’ by repetitive application of the purification protocol. Ideally, the fidelity of the remaining pair(s) can be ‘pumped’ arbitrarily close to 1, but in practice will never exceed a limit imposed by imperfections in the purification gates and the measurements used to produce the purified pairs. In addition to uses in quantum communication and large-scale quantum information processing, remote entangled atoms could be useful in more fundamental experiments, such as a loophole-free test of local hidden-variable theories. The multi-segmented trap architecture used here should allow the distribution of entangled particles to separate locations for exploring repetitive protocols in future experiments.

## METHODS

**Gate operations.** A general single-qubit rotation  $R(\theta, \phi)$  transforms the qubit states as  $R(\theta, \phi)|\uparrow\rangle = \cos(\theta/2)|\uparrow\rangle - ie^{i\phi}\sin(\theta/2)|\downarrow\rangle$ , and  $R(\theta, \phi)|\downarrow\rangle = -ie^{-i\phi}\sin(\theta/2)|\uparrow\rangle + \cos(\theta/2)|\downarrow\rangle$ . These rotations were applied uniformly to all ions that resided in the trap zone z2 addressed by the Raman laser beams (Fig. 1c–f).

Phase gates for entangling different combinations of pairs of ions in a string of four ions are a generalization of the phase gate described in ref. 16. For the arrangement of laser beams in the experiment, the phase of the dipole force repeated every 213 nm along the alignment direction of the ions. The equilibrium between mutual Coulomb repulsion and the confinement of the external trap potential determined the positions of the ions relative to the trap centre to be  $s(-1.437, -0.454, 0.454, 1.437)$ , with  $s = \sqrt{e^2/(4\pi\epsilon_0 m\omega_{\text{COM}}^2)}$ ,  $e$  the elementary charge,  $\epsilon_0$  the vacuum permittivity,  $m$  the mass of the beryllium ion and  $\omega_{\text{COM}}/(2\pi)$  the axial centre of mass (COM) frequency<sup>20</sup>. For  ${}^9\text{Be}^+$ ,  $s \approx 7.31 \mu\text{m}$  ( $\omega_{\text{COM}}/2\pi[\text{MHz}]^{-2/3}$ ). By choosing the strength of the external potential appropriately, we achieved a pattern of dipole forces that equally coupled ion 1 to 2, and ion 3 to 4, with negligible coupling of other ion pairs. Within a coupled pair, phases changed according to  $(|\uparrow\uparrow\rangle, |\uparrow\downarrow\rangle, |\downarrow\uparrow\rangle, |\downarrow\downarrow\rangle) \rightarrow (|\uparrow\uparrow\rangle, e^{i\varepsilon}|\uparrow\downarrow\rangle, e^{i\varepsilon}|\downarrow\uparrow\rangle, |\downarrow\downarrow\rangle)$ , where  $\varepsilon$  was determined by the time of the operation and the beam intensities<sup>16</sup>. To entangle two pairs of ions, we first applied a global rotation  $R(\pi/2, 0)$  to all four ions, followed by the phase gate with  $0 \leq \varepsilon \leq \pi/4$  on the axial mode at  $\omega = 2\pi \times 6.742 \text{ MHz} \approx 2.41\omega_{\text{COM}}$ , which has normalized mode amplitudes  $(\frac{1}{2}, -\frac{1}{2}, -\frac{1}{2}$  and  $\frac{1}{2})$ . We then applied a refocussing  $R(\pi, \pi)$  rotation, the same phase gate, and finally another  $R(\pi/2, 0)$  rotation. Pair preparation took less than 100  $\mu\text{s}$ . Calculations show that residual phases due to unwanted couplings only degrade the pair fidelity by 0.007. The observed loss in fidelity can be attributed to the following causes: during the pair preparation procedure, there was a 7% probability of one of the ions undergoing an absorption–spontaneous emission cycle. Phase instabilities of the single qubit rotations caused by interferometric phase fluctuations between Raman beams contributed of the order of 10% over the 1.5-ms duration of the experiment. Further imperfections included laser beam pointing and intensity noise, leading to fluctuations in the ion–laser couplings (Rabi frequencies) of the order of 5%. We also estimated an error of 5% due to fluctuations in the trapping potential, caused by noisy potentials applied to the trap electrodes. The last three errors also included systematic drifts that contributed to the statistically significant scatter in the measured fidelities (Fig. 2).

The purification gate was similar to the first gate. Two phase gates  $Z$  with angle  $\varepsilon = \pi/4$  were embedded into single qubit rotations in a sequence  $R(\pi/2, \pi/4) - Z - R(\pi, 5\pi/4) - Z - R(\pi/2, \pi/4)$  applied to all ions. The phase gates  $Z$  coupled ion 1 to 3 and 2 to 4 (see Fig. 1c) and were executed on the COM mode at a frequency of 4.07 MHz (duration 65  $\mu\text{s}$ ). Calculations show that unwanted couplings in this gate degrade the fidelity by 0.007. The actual loss of fidelity due to the purification procedure was similar to those discussed above. Additional loss of fidelity in the purified pair was caused by imperfect state discrimination of pair 1 (see main text). The photon count thresholds for inferring that exactly one ion was in state  $|\uparrow\rangle$  were set so that the probability of error is at most 5%.

**State tomography.** During detection (duration 200  $\mu\text{s}$ ) we registered between  $0.15 \leq \lambda_0 \leq 0.8$  counts if all ions are projected into  $|\uparrow\rangle$ , and between  $8 \leq \lambda_1 \leq 12$  additional average counts for each ion in state  $|\downarrow\rangle$ . Count averages  $\lambda_0$  and  $\lambda_1$  were derived by fitting mixtures of poissonian distributions to count histograms for

the relevant detection periods and to reference histograms obtained by preparing all ions to be observed in the  $|\downarrow\rangle$  or  $|\uparrow\rangle$  states. We used the maximum likelihood method for fitting the histograms, and parametric-bootstrap resampling for determining standard errors in inferred quantities<sup>21</sup>. To obtain the fidelity of the second Bell pair (ions 3 and 4), we applied the tomographic rotation  $T(\phi_a, \phi_b) = R(\pi/2, \phi_a) R(\pi/2, \phi_b)$  to both ions simultaneously, with  $\phi_a = 0, \pi/4, \pi/2$  and  $\phi_b = 0, \pi/4, \dots, 7\pi/4$ . From the photon counts obtained after the tomographic rotations, we inferred entries of the density matrix in the Bell basis before the rotations by maximum likelihood methods. The inferred entries included the Bell state populations but not the coherences between the singlet and triplet states. We used a version of the maximum likelihood algorithm described in ref. 22. In the reference experiment, we extended the tomographic inference by including the counts for the measurement of ions 1 and 2, which yielded the symmetrized density matrices on ions 3 and 4 conditional on the number of ions 1 and 2 in state  $|\uparrow\rangle$ . We used this information to check that the state in the reference experiment was consistent with the first and second pair being independently entangled. In separate experiments, we checked that the behaviour of the purification gate was consistent with correlating only ions 1 and 3, and (separately) ions 2 and 4. In both cases, we found the inferred density matrix to be consistent with the independence assumption, in the sense that they match the terms of an independent density matrix with probability of error less than 0.01.

Received 19 June; accepted 3 August 2006.

- Ekert, A. K. Quantum cryptography based on Bell's theorem. *Phys. Rev. Lett.* **67**, 661–663 (1991).
- Bennett, C. H. *et al.* Teleporting an unknown quantum state via dual classical and Einstein-Podolsky-Rosen channels. *Phys. Rev. Lett.* **70**, 1895–1899 (1993).
- Gottesman, D. & Chuang, I. L. Demonstrating the viability of universal quantum computation using teleportation and single-qubit operations. *Nature* **402**, 390–393 (1999).
- Bennett, C. H. *et al.* Purification of noisy entanglement and faithful teleportation via noisy channels. *Phys. Rev. Lett.* **76**, 722–725 (1996).
- Kwiat, P. G., Barraza-Lopez, S., Stefanov, A. & Gisin, N. Experimental entanglement distillation and 'hidden' non-locality. *Nature* **409**, 1014–1017 (2001).
- Pan, J.-W., Gasparoni, S., Ursin, R., Weihs, G. & Zeilinger, A. Experimental entanglement purification of arbitrary unknown states. *Nature* **423**, 417–422 (2003).
- Yamamoto, T., Koashi, M., Özdemir, S. K. & Imoto, N. Experimental extraction of an entangled photon pair from two identically decohered pairs. *Nature* **421**, 343–346 (2003).
- Zhao, Z., Yang, T., Chen, Y.-A., Zhang, A.-N. & Pan, J.-W. Experimental realization of entanglement concentration and a quantum repeater. *Phys. Rev. Lett.* **90**, 207901 (2003).
- Walther, P. *et al.* Quantum nonlocality obtained from local states by entanglement purification. *Phys. Rev. Lett.* **94**, 040504 (2005).
- Quantum Information Science and Technology Experts Panel. ARDA quantum information science and technology roadmap. (<http://qist.lanl.gov>) (2002).
- Browne, D. E. & Rudolph, T. Resource-efficient linear optical quantum computation. *Phys. Rev. Lett.* **95**, 010501 (2005).
- Eisert, J., Jacobs, K., Papadopoulos, P. & Plenio, M. B. Optimal local implementation of nonlocal quantum gates. *Phys. Rev. A* **62**, 052317 (2000).
- Brennen, G. K., Song, D. & Williams, C. J. Quantum computer architecture using nonlocal interactions. *Phys. Rev. A* **67**, 050302 (2003).
- Knill, E. Quantum computing with realistically noisy devices. *Nature* **434**, 39–44 (2005).
- Barrett, M. D. *et al.* Deterministic quantum teleportation of atomic qubits. *Nature* **429**, 737–739 (2004).
- Leibfried, D. *et al.* Experimental demonstration of a robust, high-fidelity geometric two ion-qubit phase gate. *Nature* **422**, 412–415 (2003).
- King, B. E. *et al.* Cooling the collective motion of trapped ions to initialize a quantum register. *Phys. Rev. Lett.* **81**, 1525–1528 (1998).
- Ozeri, R. *et al.* Hyperfine coherence in the presence of spontaneous photon scattering. *Phys. Rev. Lett.* **95**, 030403 (2005).
- Barrett, M. D. *et al.* Sympathetic cooling of  $^9\text{Be}^+$  and  $^{24}\text{Mg}^+$  for quantum logic. *Phys. Rev. A* **68**, 042302 (2003).
- Wineland, D. J. *et al.* Experimental issues in coherent quantum-state manipulation of trapped atomic ions. *J. Res. Nat. Inst. Stand. Technol.* **103**, 259–328 (1998).
- Efron, B. & Tibshirani, R. J. *An Introduction to the Bootstrap* (Chapman & Hall, New York, 1993).
- Lvovsky, A. I. & Raymer, M. G. Continuous-variable optical quantum state tomography. Preprint at (<http://www.arXiv.org/quant-ph/0511044>) (2005).

**Acknowledgements** This work was supported by the Disruptive Technology Office (DTO), by a DoD Multidisciplinary University Research Initiative (MURI) programme administered by the Office of Naval Research and by NIST. R.R. was supported by the Alexander von Humboldt Foundation. We thank S. Glancy and W. Itano for comments on the manuscript.

**Author Information** Reprints and permissions information is available at [www.nature.com/reprints](http://www.nature.com/reprints). The authors declare no competing financial interests. Correspondence and requests for materials should be addressed to D.L. ([dil@boulder.nist.gov](mailto:dil@boulder.nist.gov)).